Surface anharmonicity on Cu(110)

Georges Armand
Service de Physique des Atomes et des Surfaces, Centre d'Etudes Nucléaires de Saclay, 91191 Gif-sur-Yvette CEDEX, France

Peter Zeppenfeld
Institut für Grenzflächenforschung und Vakuumphysik, Kernforschungsanlage Jülich, Postfach 1913, D-5170 Jülich, West Germany

(Received 1 March 1989)

Using high-resolution He-atom scattering, we have measured the thermal attenuation of the specular beam and the variation of the inelastically scattered one-phonon and multiphonon intensities as a function of temperature. A dynamical calculation including transition matrix elements up to third order, and taking into account a strongly enhanced surface anharmonicity, describes both the specular- and the inelastic-scattering data.

I. INTRODUCTION

The thermal behavior of crystal surfaces has recently attracted much interest. Theoretical and experimental studies dealing with phenomena such as surface roughening[1–4] and surface melting[5–8] have revealed the important role played by the surface with respect to the thermal stability of crystals: for instance, melting has been shown to be a "surface-initiated" process.[5–8] In this context the investigation of the dynamics of the surface atoms as a function of temperature will provide additional information on the thermal properties of surfaces. A dynamical calculation for the low-index Cu surfaces revealed a larger increase in the mean-square vibrational amplitude of the surface atoms with temperature as compared to the bulk values.[5] It was argued that this may indeed give rise to a surface-initiated melting. Experimentally, the surface melting of Pb(110) occurring at $T\sim 545$ K has been observed to be preceded by an anomalous increase of the thermal-expansion coefficient already above 400 K,[9] which was then ascribed to an increased surface anharmonicity. Likewise, investigations of different Cu and Ni faces showed a large increase in the mean-square displacement of the surface atoms for temperatures well below the roughening transition or the melting temperature.[10,11]

More recently, the morphology of the Cu(110) surface has been studied by means of high-resolution He-atom diffraction for different temperatures $T\leq 900$ K.[12] An enhanced decrease of the specular and higher-order diffraction peaks has been observed. A detailed analysis of the widths and line shapes of the diffraction peaks, however, shows no evidence for the formation of terraces (roughening transition) or a loss of long-range order (melting) up to 900 K. Furthermore, the diffusely elastic scattered He intensity, being a sensitive measure of surface defects such as adatoms, steps, or impurity atoms,[13] continuously decreases, indicating that surface defects cannot be the main cause for the observed enhanced decrease of the specular intensity. Therefore, this enhanced decrease of intensity has been tentatively interpreted as being due to an enhanced surface anharmonicity, as also proposed earlier in the case of Cu(100).[10]

The purpose of this paper is to verify to what extent this assumption is realistic as far as the (110) face is concerned. In this aim we compare the temperature dependence of the measured specular intensity and of the experimental one-phonon and multiphonon cross sections to calculated values taking into account anharmonic effects. The cross-section values are calculated with matrix elements up to third order in the perturbation expansion, i.e., well beyond the distorted-wave Born approximation (DWBA). The validity of the calculated results is then extended beyond the very-low-temperature region.

II. THEORY

Let us consider an incident particle in a state i (energy E_i) scattered by the surface potential in a state f (energy E_f). The transition rate ${}_fw_i$ is given by the expression

$$ {}_fw_i=\frac{1}{\hbar^2}\int_{-\infty}^{+\infty}\exp\left[\frac{i\lambda}{\hbar}(E_f-E_i)\right] \times\langle\langle {}_iT_f^{\dagger}(0)\,{}_fT_i(\lambda)\rangle\rangle d\lambda\ , \tag{1}$$

in which the angular brackets stand for a thermal average over the crystal phonon field. T is the matrix element taken between the initial and final particle states, calculated with the T matrix equation

$$T=V(\mathbf{R},z,\mathbf{u})-\langle\langle V\rangle\rangle+[V(\mathbf{R},z,\mathbf{u})-\langle\langle V\rangle\rangle]G^{+}T\ . \tag{2}$$

V is the particle crystal potential, depending upon the particle coordinates $\mathbf{R},z$ and on its thermal displacement $\mathbf{u}$. With $v\equiv V-\langle\langle V\rangle\rangle$ the iteration of Eq. (2) gives

$$T=v+vG^{+}v+vG^{+}vG^{+}v+\cdots\ , \tag{3}$$

where the inclusion of the leading terms is associated, respectively, with perturbation orders 1,2,3, ... Replacing T by the expansion (3) in Eq. (1) one gets

TABLE I. Matrix elements included in the calculation using the perturbation expansion up to third order.

	Number of matrix elements	Number of real phonons	Proportional to
$\langle\langle 1^+1\rangle\rangle$	1	1	T
	1	2	T^2
$\langle\langle 1^+2\rangle\rangle+\langle\langle 2^+1\rangle\rangle$	2	1	T^2
	1	2	T^2
$\langle\langle 1^+3\rangle\rangle+\langle\langle 3^+1\rangle\rangle$	3	1	T^2
$+\langle\langle 2^+2\rangle\rangle$	2	2	T^2

$$\langle\langle {}_iT_f^\dagger(0)\,{}_fT_i(\lambda)\rangle\rangle=\langle\langle {}_iv_f^\dagger(0)\,{}_fv_i(\lambda)\rangle\rangle+\langle\langle {}_iv_f^\dagger(0)\,{}_f[v(\lambda)G^+v(\lambda)]_i\rangle\rangle+\cdots,$$

or in short-hand form, using the perturbation-order notation,

$$\langle\langle {}_iT_f(0)\,{}_fT_i(\lambda)\rangle\rangle=\langle\langle 1^+1\rangle\rangle+\langle\langle 1^+2\rangle\rangle+\langle\langle 2^+1\rangle\rangle+\langle\langle 1^+3\rangle\rangle+\cdots.$$

In each of these terms the thermal average yields an exponential of the correlation function $\langle\langle u(0)u(\lambda)\rangle\rangle$, which after expansion gives the matrix elements describing the exchange of 1,2, . . . , n phonons. The detailed analysis is given elsewhere.[14] The results are summarized in Table I, which gives the number of matrix elements proportional to the crystal temperature T (DWBA) or to T^2, corresponding to the exchange of one and two phonons, respectively. All other matrix elements coming from higher-order terms in the expansion are at least proportional to T^3.

The matrix elements of Table I have been included in the numerical calculation, and the results quoted below therefore contain all contributions to the inelastic events proportional to T and T^2. The potential between the incident particle and the crystal is taken equal to

$$V=D\{\exp[-2\chi(z-u)]/v_0-2\exp(-\chi z)\}\ , \qquad (4)$$

where $v_0\equiv\langle\langle V\rangle\rangle$, D being the well depth and χ the potential stiffness.

This potential has been successfully used to calculate the thermal attenuation of the specular beam in the case of the (100) face of copper. Its properties as well as the relevant values of the physical parameters are discussed elsewhere.[10] For the present calculation we further used the total spectral density for the atoms of the (110) face calculated in the same way as for the (100) face.

V given by expression (4) is a one-dimensional potential and consequently all the particles are scattered in the incident plane with conservation of the momentum component parallel to the surface. Therefore the calculated reflection coefficient (${}_fR_i={}_fw_i$ divided by the incident flux) for the one- and two-phonon exchange will be greater than the measured one. However, such a calculation can yield the correct dependence of these intensities on crystal temperature; this will be the matter of comparison to the experimental data. The specular-beam intensity I_0 has been calculated using a procedure which includes the multiphonon processes.[15]

III. EXPERIMENT

We have measured the energy distribution of He atoms scattered from the clean Cu(110) face as a function of surface temperature for different scattering conditions. Using a primary He-beam energy of 18.3 meV, we changed the scattering conditions by varying the incident and outgoing angles ϑ_i and ϑ_f, respectively; however, this was done with the constraint $\vartheta_i+\vartheta_f=90°$ imposed by our apparatus. For a detailed description of the He-scattering apparatus the reader is referred to Ref. 16. The misorientation and the residual mosaic of the Cu(110) crystal were less than 0.2°. The sample was cleaned *in situ* by successive cycles of heating and Ar-ion sputtering.

Using the pseudorandom time-of-flight technique,[16] we have analyzed the energy distribution of the He atoms scattered from the Cu(110) surface, and three contributions to the total (diffusely) scattered intensity could be distinguished, as shown in Fig. 1: (a) a narrow, purely

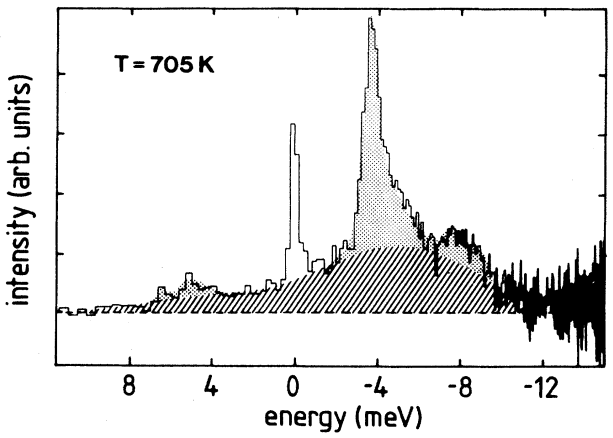

FIG. 1. Energy spectrum of He atoms scattered from the Cu(110) surface along the [001] direction at a surface temperature $T=705$ K (incident beam energy and angle 18.3 meV and 40°, respectively). The peak at zero energy transfer corresponds to He atoms scattered from residual defects on the surface. The dotted area originates from one-phonon inelastic-scattering events while the broad background (hatched area) can be attributed to multiphonon scattering.

elastic peak, (b) sharply structured one-phonon gain and loss features at well-defined exchange energies, (c) a broad, smoothly varying background [on which contributions (a) and (b) are superimposed], which may be attributed to multiphonon excitation. Since all three contributions can be easily separated from each other, the diffuse elastic, the one-phonon, and the multiphonon intensities can be straightforwardly evaluated from the area below the appropriate signals.

IV. RESULTS AND DISCUSSION

The specularly reflected He intensity has been measured for different crystal temperatures independently in two different experiments[12,17] [see inset of Fig. 2(a)], and compared to the calculated values assuming a harmonic crystal (Debye temperature $\Theta_D = 350$ K). The measured values are lower than the calculated ones and the difference, which is small at low temperature, increases rapidly above 550 K. Anharmonicity is introduced in the calculation through the quasiharmonic scheme by a variation of the crystal maximum frequency Ω_m with crystal temperature. This frequency is adjusted for every temperature in such a way that the calculated intensity fits the experimental data. The procedure has been previously described and applied to the case of the Cu(100) face.[10] The results are shown in Fig. 2(a), where, instead of Ω_m, the mean-square displacement normal to the surface of a surface atom is plotted versus crystal temperature. Note that both data sets[12,17] can be fitted using the same values for the mean-square displacement of the surface atoms. For a comparison the corresponding curves for the copper (100) face[10] and for bulk atoms are also plotted. At high temperature the surface anharmonicity on the (110) face appears to be strongly enhanced compared to that of the (100) face. However, quantitative results obtained within the quasiharmonic approximation should be considered with some care, especially when the anharmonic effects are very strong. Hence, in the high-temperature region the difference between the two faces might be overestimated.

The temperature dependence of the measured and calculated one-phonon and multiphonon cross-section values is shown in Fig. 2(b). A significant change is obtained when one takes into account the surface anharmonicity as determined above. Note that the experimen-

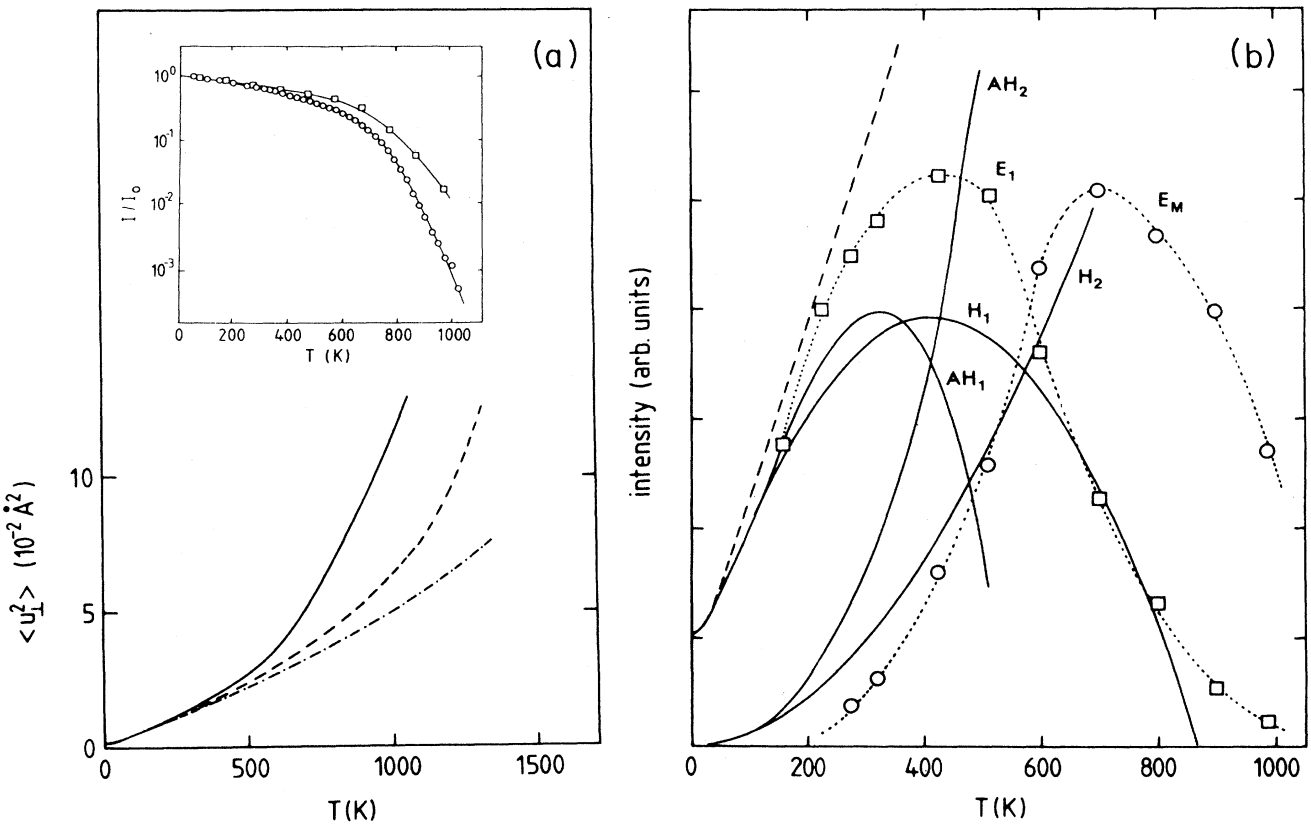

FIG. 2. (a) Perpendicular mean-square displacement of a surface atom: with bulk anharmonicity (dashed-dotted line), for the Cu(100) face (Ref. 10) (dashed line), and for the Cu(110) face (solid line) fitted to the measured specular beam intensity for two different experimental data sets as shown in the inset. □: $E_i = 21$ meV, $\vartheta_i = \vartheta_i = 67.4°$ (Ref. 17). ○: $E_i = 18.3$ meV, $\vartheta_i = \vartheta_f = 45°$ (Ref. 12). (b) E_1, E_M, measured cross sections for the one-phonon and multiphonon exchange, respectively. H_1, H_2, AH_1, AH_2, calculated cross-section values for one- and two-phonon exchange: H, harmonic crystal; AH, with Cu(110) surface anharmonicity corresponding to Fig. 2(a). Dashed line: one-phonon exchange calculated in the DWBA. Incident energy 18.3 meV, incident angle $\vartheta_i = 40°$, final-state angle $\vartheta_f = 50°$.

tal data have been scaled in such a way that the measured one-phonon cross section for $T=100$ K coincides with the calculated one at this temperature. Clearly, the general features of the experimental data are well reproduced by the calculation: the contribution of the matrix elements proportional to T^2 yields a maximum on the one-phonon curve. The same feature would appear on the two-phonon curve if we could add the contribution of the matrix elements proportional to T^3.

Let us emphasize here a—at first sight embarrassing—feature of the experimental data: they seem to violate unitarity. Indeed for $T \geq 650$ K both the total diffuse intensity (elastic and inelastic) and the coherent elastic one (specular and diffraction peaks) decrease. All measurements having been performed so far in plane, the unitarity has to be reestablished by an increase of the out-of-plane multiphonon scattering. This idea is supported by experiment: at larger parallel momentum transfer, as well as when scattering along nonsymmetry directions, the multiphonon intensity exhibits no maximum but steadily increased up to the highest temperature measured (900 K). Note that under these conditions the one-phonon intensity is drastically reduced. A detailed study of the spatial distribution of the inelastic-scattered intensity would therefore be of great interest; however, this is a difficult task. The experiments will in general suffer from their restricted scattering geometry; theoretically, the models used so far for accurately calculating multiphonon scattering intensities are strictly one dimensional.

At first inspection, the harmonic calculation seems to give better results with respect to the experimental data. However, before drawing a conclusion it is necessary to determine the temperature range in which the calculated curves are valid, and to estimate the influence of the terms proportional to T^3. This can be done by comparing the total inelastic reflection coefficient I_{inel} (i.e., in the approximation used, the sum of the one- and two-phonon terms proportional to T an T^2) to $1-I_0$, where I_0 is the calculated specular intensity. Figure 3 gives the comparison for the case of a harmonic crystal. The difference between these two quantities is very small below 250 K, increases with temperature, and becomes important above 600 K. Including surface anharmonicity, these two temperatures are lowered and can be estimated to be equal to 200 and 450 K, respectively. Hence the influence of the matrix elements proportional to $T^3, T^4, \ldots$ can be evaluated. Their contributions yield an increase of the whole inelastic cross section. However, their influence on the one- and two-phonon intensities will be different: for the former, the matrix elements proportional to T^3 will produce a progressive increase of this cross section. For the latter, they will yield a reverse effect leading eventually to a decrease, i.e., to the appearance of a maximum as pointed out above. The contribution of matrix elements proportional to $T^4, \ldots$ will cause the one-phonon intensity to reach a maximum and then decrease to zero, while the multiphonon contribution will approach the unitarity limit at high T. However, the T^3 terms yield the main correction in the temperature range 200–600 K, and when this correction is included the anharmonic curves can be expected to give a better representation of the experimental data in this range. As already noted, the observed decrease of the multiphonon intensity at high temperature can be explained by a redistribution of the scattering towards out-of-plane angles for processes involving more than two phonons. It is then reasonable to compare the experimental curve E_M with the calculated two-phonon intensity alone, as we have done.

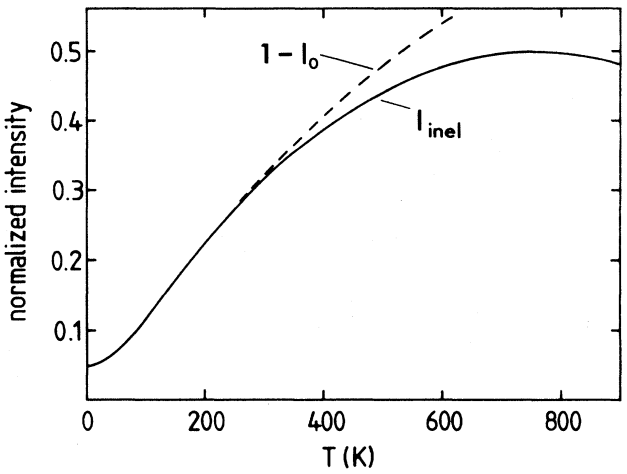

FIG. 3. I_{inel} total reflection coefficient calculated with matrix elements in Table I. $1-I_0$: total inelastic scattering with I_0 the calculated specular intensity. Incident beam energy and angle 18.3 meV and 40°, respectively.

V. CONCLUSIONS

The analysis of elastic and inelastic experimental data strongly supports the hypothesis of an enhanced surface anharmonicity on the (110) face of copper, which would be more important at high temperature than that of the (100) face deduced from similar experiments. Nevertheless, this enhancement does not exclude the formation of a small amount of disorder, such as, for example, the "missing-row" type disorder.[18] Furthermore, we have shown that a cross-section calculation which includes only the DWBA matrix elements cannot give a good representation of the experimental data.

[1]J. Villain, D. R. Grempel, and J. Lapujoulade, J. Phys. F **15**, 809 (1985).

[2]M. den Nijs, E. K. Riedel, E. H. Conrad, and T. Engel, Phys. Rev. Lett. **55**, 1689 (1985); **57**, 1279(E) (1986).

[3]E. H. Conrad, R. M. Aten, D. S. Kaufman, L. R. Allen, T. Engel, M. den Nijs, and E. Riedel, J. Chem. Phys. **84**, 1015 (1986); **85**, 4756(E) (1986).

[4]F. Fabre, D. Gorse, B. Salanon, and J. Lapujoulade, J. Phys. (Paris) **48**, 1017 (1987).

[5]C. S. Jayanthi, E. Tosatti, and L. Pietronero, Phys. Rev. B **31**, 3456 (1985).

[6]A. Trayanov and E. Tosatti, Phys. Rev. Lett. **59**, 2207 (1987).

[7]J. W. M. Frenken and J. F. van der Veen, Phys. Rev. Lett. **54**, 134 (1985); J. W. M. Frenken, P. M. J. Maree, and J. F. van

der Veen, Phys. Rev. B **34**, 7506 (1986).
[8]K. C. Prince, U. Breuer, and H. P. Bonzel, Phys. Rev. Lett. **60**, 1146 (1988).
[9]J. W. M. Frenken, F. Huussen, and J. F. van der Veen, Phys. Rev. Lett. **58**, 401 (1987).
[10]G. Armand, D. Gorse, J. Lapujoulade, and J. R. Manson, Europhys. Lett. **3**, 1113 (1987).
[11]E. H. Conrad, L. R. Allen, D. L. Blanchard, and T. Engel, Surf. Sci. **198**, 207 (1988).
[12]P. Zeppenfeld, K. Kern, R. David, and G. Comsa, Phys. Rev. Lett. **62**, 63 (1989).
[13]A. M. Lahee, J. R. Manson, J. P. Toennies, and Ch. Wöll, Phys. Rev. Lett. **57**, 471 (1986); **57**, 2331(E) (1986); A. M. Lahee, J. R. Manson, J. P. Toennies, and Ch. Wöll, J. Chem. Phys. **86**, 7194 (1987); J. R. Manson, Phys. Rev. B **37**, 6750 (1988).
[14]G. Armand, J. Phys. (Paris) **50**, 1493 (1989).
[15]G. Armand, J. R. Manson, and C. S. Jayanthi, Phys. Rev. B **34**, 6627 (1986).
[16]R. David, K. Kern, P. Zeppenfeld, and G. Comsa, Rev. Sci. Instrum. **57**, 2771 (1986).
[17]D. Gorse and J. Lapujoulade, Surf. Sci. **162**, 847 (1985).
[18]A. Trayanov, A. C. Levi, and E. Tosatti (unpublished).